April 15, 2011

Oscillatory glucose flux in INS 1 pancreatic β cells: A self-referencing microbiosensor study

Jin Shi, *Purdue University*
Eric S. McLamore, *Purdue University*
David B. Jaroch, *Purdue University*
Jonathan C. Claussen, *Purdue University*
Raghavendra G. Mirmira, *Indiana University School of Medicine*, et al.

Published in final edited form as:
Anal Biochem. 2011 April 15; 411(2): 185–193. doi:10.1016/j.ab.2010.12.019.

Oscillatory glucose flux in INS 1 pancreatic β cells: A self-referencing microbiosensor study

Jin Shi[1,2,3], **Eric S. McLamore**[1,2,4], **David Jaroch**[1,2,3], **Jonathan C. Claussen**[1,2,4], **Jenna L. Rickus**[1,2,3,4], and **D. Marshall Porterfield**[1,2,3,4,5,†]

[1]Physiological Sensing Facility 1203 W. State Street, Purdue University, West Lafayette, IN 47907-2057

[2]Birck Nanotechnology Center and Bindley Bioscience Center 1203 W. State Street, Purdue University, West Lafayette, IN 47907-2057

[3]Weldon School of Biomedical Engineering 1203 W. State Street, Purdue University, West Lafayette, IN 47907-2057

[4]Department of Agricultural and Biological Engineering 1203 W. State Street, Purdue University, West Lafayette, IN 47907-2057

[5]Department of Horticulture & Landscape Architecture 1203 W. State Street, Purdue University, West Lafayette, IN 47907-2057

Abstract

Signaling and insulin secretion in β cells have been reported to demonstrate oscillatory modes, with abnormal oscillations associated with type 2 diabetes. We investigated cellular glucose influx in β cells with a self-referencing microbiosensor based on nanomaterials with enhanced performance. Dose-response analysis with glucose and metabolic inhibition studies were used to study oscillatory pattern and transporter kinetics. For the first time, we report a stable and regular oscillatory uptake of glucose (averaged period 2.9±0.6minutes), which corresponds well with an oscillator model. This oscillatory behavior is part of the feedback control pathway involving oxygen, cytosolic Ca^{2+}/ATP, and insulin secretion (periodicity approximately 3 minutes). Glucose stimulation experiments show that the net Michaelis-Menten constant (6.1±1.5mM) is in between GLUT2 and GLUT9. Phloretin inhibition experiments show an EC_{50} value of 28±1.6μM-phloretin for class I GLUT proteins and a concentration of 40±0.6μM-phloretin caused maximum inhibition with residual non-oscillating flux, suggesting that the transporters not inhibited by phloretin are likely responsible for the remaining non-oscillatory uptake, and that impaired uptake via GLUT2 may be the cause of the oscillation loss in type 2 diabetes. Transporter studies using the SR microbiosensor will contribute to diabetes research and therapy development by exploring the nature of oscillatory transport mechanisms.

Keywords

glucose oxidase; biosensor; self referencing; diabetes; glycolysis; β cell

[†]Corresponding author (tel: 765-494-1190; fax: 765-496-1115; porterf@purdue.edu) .

Introductory Statement

Glucose plays a central role in metabolism, and glucose transport is commonly studied in cancer research (e.g., Wharburg effect), diabetes, and other cell/tissue culture applications. Changes in glucose transport are particularly critical in diabetes research. β cells in the mammalian pancreas secrete insulin [1; 2], and according to the consensus model (triggering pathway) [3; 4], glucose enters β cells via glucose transporters (GLUT), and is catabolized (glycolysis, TCA, mitochondrial respiration) to produce ATP. Increased intracellular ATP closes plasmalemma K_{ATP} channels, which depolarizes the membrane and opens voltage dependent Ca^{2+} channels. This influx of Ca^{2+} triggers the docking of insulin vesicles and exocytosis. Subsequent studies have shown that when cytosolic Ca^{2+} increases through the triggering pathway, an amplifying pathway is initiated, increasing efficacy of Ca^{2+} on exocytosis of insulin granules [5].

Ca^{2+}/ATP signaling and insulin secretion in β cells exhibit an oscillatory mode [3; 4]. The link between insulin secretion, glucose, oxygen, calcium and ATP in pancreatic β cells has led to the development of numerous feedback models, for example, increased intracellular Ca^{2+} stimulates ATP consumption, reducing ATP/ADP ratio, and inducing the reopening of the K_{ATP} channels and the decrease of Ca^{2+} influx [6]. Other explanations of the oscillatory mechanisms include oscillatory glycolysis theory [7], multi-system theory [8], phase control and modulation theory [9], and the dual oscillator model [10]. Similar periods (around 3 min) have been reported for oxygen influx, cytosolic Ca^{2+}, the ATP/ADP ratio, and insulin secretion [3; 11; 12; 13; 14]. Since oscillations correlate with insulin secretion [7], and the oscillatory secretion of insulin is lost in both individuals with type 2 diabetes and their near relatives due to defective temporal coordination of β cell function [15; 16; 17], research on oscillation patterns have garnered significant interest [1; 2; 3; 7; 11].

GLUT2 is the main glucose transporter documented in mouse pancreatic β cells [18]. However, some studies on glucose uptake and the maintenance of second phase insulin secretion in GLUT2-null islets suggest the existence of an unidentified GLUT transporter other than GLUT1 or GLUT3 [19]. Following studies have subsequently reported that GLUT9 may be the unidentified transporter that participates in the regulation of glucose homeostasis in addition to GLUT2 [20]. Since mutations in the *IPF1/PDX1* gene cause the development of type 2 diabetes, impaired expression of GLUT2 and impaired secretion of insulin [21], abnormalities in glucose transport may be related to the cause of type 2 diabetes. Thus, studies on transporter kinetics and the pharmacological modulation may provide further insight into type 2 diabetes.

A number of techniques have been used for measuring glucose concentration in cells/tissues to understand these transport phenomena. These include $^{14}CO_2$ radioactivity from [U-^{14}C] glucose [22], $^{3}H_2O$ from [5-^{3}H] glucose [19], ^{13}C NMR spectroscopy [23], and microfluorometry assays of 6-phosphogluconate [24]. All these techniques are complex and invasive (requiring extraction). Thus, there is now a need for sensitive tools which can directly quantify glucose transport in the cell/tissue spatial domain under physiological conditions.

Glucose biosensors are based on enzymatic recognition of glucose by glucose oxidase (GOx), where oxidation to gluconic acid produces H_2O_2, which is detected using oxidative amperometry at a potential of +0.3-0.8V [25]. Based on the highly specific enzymatic recognition scheme, glucose biosensors do not respond to other sugar moieties such as sucrose or fructose [26]. In addition, since the RPMI culture media for INS 1 contain no sugar moieties other than glucose, the output signal is completely due to glucose oxidation. Thus, the selectivity of glucose biosensors is ensured. Enzyme based electrochemical

glucose biosensors have demonstrated important applications in measuring glucose; e.g., in single islets [27] for research. Many of these studies are aimed at enhancing understanding of fundamental cell biology, and/or improving the design of point of care diagnostics. In addition to the development of enzyme based glucose biosensors, many researchers have focused on enhancement of these tools with various nanomaterials [25; 28].

Conductive carbon nanotubes (CNTs) are a nanomaterial which improve biosensor performance by enhanced electrochemical transduction and/or increased enzyme loading [29]. The major difficulty for CNT immobilization is that CNTs are highly insoluble due to aggregation via van der Waals forces among tubes [29]. CNT immobilization approaches using polymers that can suspend CNTs are the most commonly used. In particular Nafion has received a lot of attention due to superior conductivity, chemical and mechanical stabilities, strong adhesion to electrode surfaces and a low swelling capability in aqueous media [29; 30]. In addition to CNTs, metal nanomaterials such as Pt black are commonly used to increase electrochemical transduction and electrode effective surface area [31]. Combining CNTs and metal nanomaterials has proved to be a valuable approach for improving biosensor performance [25; 28; 32].

Although a wealth of knowledge has been gained regarding the use of GOx micro biosensors incorporating various CNT/nanomaterials, most devices are prone to high drift/noise when used for analyzing glucose concentrations near cells/tissues under physiological conditions [33]. In addition, concentration measurements using classic microsensor techniques are not capable of quantifying the direction of transport (i.e., flux) [30]. A microsensor technique developed to improve the signal-to-noise ratio and provide direct measurement of transmembrane flux is known as self-referencing (SR) [30; 33; 34]. The SR microsensor technique has been used extensively to study important biological phenomena [35; 36; 37; 38]. SR is based on Fick's first law of diffusion, and involves measurement of concentration gradients (ΔC) during oscillatory movement of a microsensor between two positions separated by a fixed distance (ΔX):

$$J=D\frac{\Delta C}{\Delta X}=D\frac{\Delta I}{k\Delta X}$$

where J is the analyte flux, D is the molecular diffusion coefficient for glucose, ΔC is the measured concentration differential, ΔX is the distance between the two measurement positions (30 μm), k is the amperometric sensitivity of the biosensor, and ΔI is the differential measured current output at 500mV.

This work presents a novel self-referencing Pt black/MWNT/Nafion/GOx glucose micro biosensor (bionanocomposite sensor) fabricated from a Pt/Ir microelectrode for direct measurement of glucose flux under physiological conditions. The biosensor was specifically designed to ensure that islet/β cell physiology was not affected by biosensor operation, and that no physical damage to the bionanocomposite layer occurred (which may potentially occur during *in vivo* experimentation). The technique was used to measure glucose influx in cultured β cells under a wide range of physiological and pathophysiological conditions to study transport patterns, transporter kinetics and the pharmacological effects of inhibitors on glucose transport.

Materials and Methods

Chemicals and reagents

Deionized water (DI) of resistivity 18.2 MΩ cm (Milli Q) was used to prepare solutions. PBS (pH 7.4), glucose oxidase (E.C.1.1.3.4, 100,000-250,000 units/g, from *Aspergillus niger*), potassium chloride (KCl, 99%), potassium ferricyanide ($K_3Fe(CN)_6$), Nafion (5% *wt*/*wt*), chloroplatinic acid solution (8% *wt*/*wt*), lead acetate (reagent grade, 95%), phloretin, β mercaptoethanol, HEPES buffer, sodium pyruvate, glutamine, penicillin and streptomycin were purchased from Sigma Aldrich (St. Louis, MO). D-Glucose and sodium chloride (NaCl) were purchased from Mallinckrodt Baker, Inc (Phillipsburg, NJ). Sodium phosphate ($Na_2HPO_4{\cdot}7H_2O$), potassium phosphate (KH_2PO_4, monobasic) and potassium cyanide (KCN) were purchased from Fisher chemicals (Pittsburg, PA). MWNTs (-COOH Functionalized MWNTs, 95 wt%, 8-15nm outside diameter) were purchased from Cheap Tubes, Inc. (Brattleboro, VT). RPMI 1640 medium was purchased from GIBCO (Carlsbad, CA), and fetal calf serum was purchased from Invitrogen (Carlsbad, CA),

Construction of bionanocomposite sensor

If not specified, all sensor development experiments were carried out at room temperature. Pt black was electrodeposited on a Pt/Ir microelectrode (PI20033.0A10 Microprobe. Inc, 1-2μm tip diameter) using a potentiostat (Applicable Electronics) against a bare Pt wire (0.5mm in diameter; Alfa Aesar, Ward Hill, MA) in a solution of 0.72% chloroplatinic acid and 0.001% lead acetate (10V for 1 minute). A MWNT solution containing 2mg MWNT/ml Nafion was ultrasonicated for 120 minutes. Two μl MWNT solution was cast on the tip of the microelectrode using a pipette. The microelectrode was air dried for 5 minutes, and then dipped in 100 μl 50 mg GOx/ml PBS for 30 min at 4°C, and stored in the same solution at 4°C when not in use.

Sensor Calibration

Cyclic voltammetry (CV) (a sweeping potential was applied to the electrode, and the current was recorded) and DC potential amperometry (a constant potential was applied to the electrode, and the current response was recorded) were carried out with a 3 electrode electrochemical (C-3) cell stand (BASi, West Lafayette, IN) and sensors calibrated according to published techniques [32].

Imaging

All field emission scanning electron microscopy (FESEM) graphs of the biosensor were obtained from a Hitachi S-4800 microscope with a power setting of 5.0kV and magnification settings of 3.5k and 25k.

Cell viability

Cell viability was evaluated using a combination of CellTracker (CellTracker Green CMFGA; Invitrogen Molecular Probes, Carlsbad, CA) and propidium iodide (PI) (Invitrogen Molecular Probes, Carlsbad, CA) cell stains. Living cells with active intercellular esterase activity stain green with CellTracker while cells with damaged membranes stain red with PI. INS 1 cells were donated by Dr. Raghu Mirmira, and were originally isolated from a transplantable rat insulinoma induced by X ray [39]. INS 1 cells were cultured in growth medium with 10 μM of CellTracter for 40 min, and for an additional 30 minutes after culture media was refreshed. The growth media was aspirated and PBS containing 0.01 mg/ml PI was introduced. Cells were then imaged within 30 minutes using an Olympus IX81 confocal microscope equipped multi-wavelength lasers (488 and 514nm) and Fluoview FV100 software for image capture.

Self Referencing

The SR system has been described previously [33]. Automated Scanning Electrode Technique (ASET) software (Science Wares, Falmouth, MA) and A/D (analog-to-digital) board with DC coupled differential amplifier, low/high pass filters, and video/data acquisition system (Applicable Electronics, Inc., Sandwich, MA) were used. Preamplifier signals were coupled through offset function to discretely subtract off baseline signals (DC coupling) to allow the differential waveform to be sufficiently amplified for digital analysis of the differential signals [33].

For abiotic validation of glucose flux measurements at 37°C, a solution containing 3 mM glucose and 0.5% agar was heated to gel, mixed, injected into a pulled micropipette (tip diameter 50 μm) and allowed to cool at room temperature. The micropipette was mounted and submersed in PBS at 37°C and 30 minutes were allowed to create a stable steady-state abiotic glucose concentration gradient near the pipette tip. The microbiosensor was positioned at tip surface, and flux was measured by oscillating biosensor at suggested frequency [40] perpendicular to the tangent of the tip surface to prevent mixing and ensure optimal performance. Following minimum nine measurements, sensor was positioned 5 μm from tip surface, and flux again recorded. This step back process was repeated until no change (<1%) in glucose efflux was observed. An empirical model was developed based on concentration measurements for describing the flux, and the correlation coefficient between the measured and predicted flux was calculated to describe the performance of SR biosensor [33; 34; 36].

INS 1 cell culture and in vitro tests

INS 1 cells were cultured on 10 cm BD Falcon polystyrene tissue culture dishes (VWR, West Chester, PA) in RPMI 1640 medium, 10% fetal calf serum, 50 μmol/l β mercaptoethanol, 10 mmol/l HEPES, 1 mmol/l sodium pyruvate, 2 mmol/l L-glutamine, 100 U/ml of penicillin, and 100 μg/ml streptomycin. Cultured cells were detached from culture dishes with 0.05% trypsin EDTA solution when 90% confluency was reached. After centrifugation, the cells were suspended in 4 ml culture media. Suspended cells were deposited on a 10 cm tissue culture plate (VWR) using a pipette to form cell rich droplets (4 droplets per plate at different places, 250 μl per drop, seeding density 1 million cells/ml), and incubated for 2 hours to allow for cellular attachment. Culture media (10ml) was added to each dish and cells were incubated for 12 hours before all *in vitro* experiments. All i*n vitro* tests were conducted on monolayer cultures of attached INS 1 cells incubated in culture media at 37°C. For flux measurements, a glucose microbiosensor was positioned at the surface (distance less than 1 μm) of cell clusters using the video zoomscope as previously described [30]. Prior to each experiment a background measurement (reference) was taken 3 mm from the β cell cluster surface for a minimum of 5 min (null internal control). For all experiments, glucose flux was continuously measured at the surface of cells for a minimum of 30 minutes prior to stimulation/inhibition. Steady state flux was defined as either < 3% change in oscillation period, or < 3% change in flux. As an external control, all experiments were repeated in the absence of cells (sterile media) using the same protocol at 37°C.

Results and Discussion

Self-referencing biosensor characterization

Cyclic voltammetry (CV) was carried out for characterization of electrochemical behavior on a bare Pt/Ir microelectrode, and a bionanocomposite micro biosensor in $Fe(CN)_6^{3-}$ from 0 to +650 mV at a scan rate 20 mV/sec (Fig. 1a). The CV for the bare electrode exhibited a sigmoid curve and steady state diffusion-limited current, which is characteristic of

microelectrodes [41]. In addition to enhanced current, the bionanocomposite sensor also exhibited non-steady state diffusion-limited characteristics, likely due to the high film resistance of the MWNT/Nafion layer [28]. Diffusion limited current is defined as $i_{lim} = KnFDCr$ [41], where i_{lim} is the diffusion-limited current, K is a geometric constant ($K=2\pi$ for hemispherical diffusion model), n is the number of electrons transferred during the redox of $Fe(CN)_6^{3-}$, F is the faradic constant, D is the diffusion coefficient for potassium ferricyanide ($6.70\pm0.02\times10^{-6}$ cm^2/s), C is the concentration of potassium ferricyanide (4 mM) and r is the microelectrode tip radius.

Based on this equation, the ratio of electrode tip radius between the nanomaterial modified biosensor and the bare electrode was estimated to be 11.5. This increase in effective surface area (i.e., tip radius measured via CV) is attributed to the deposition of catalytic nanomaterials [28]. Based on FESEM, low (inset approximately 60 × 40μm) and high magnification images demonstrated the deposition of homogeneous Pt black and MWNT layers (Fig. 1b&c). Pt black nanostructures were composed of a continuous film of amorphous Pt nanoclusters, and the MWNT matrix provided a highly porous matrix for immobilization of glucose oxidase via both covalent bonding (bovine serum albumin-glutaraldehyde linkages) and absorption, which was validated in previous studies [42; 43].

As expected, calibration at 37°C via DC potential amperometry (+500mV) indicated significantly higher H_2O_2 sensitivity for the bionanocomposite sensor compared with bare Pt electrode (Fig. 2 a&b). Since enzymes were immobilized on the biosensor via dip coating and there was not an established method to determine the amount of enzymes immobilized on biosensors, it was difficult to specify the yield of glucose oxidase immobilization in terms of enzyme loading. Instead, the accepted convention was to characterize the amperometric sensitivity to glucose [32; 44]. Bionanocomposite sensors exhibited a well defined linear response towards glucose with a sensitivity of 531±149 pA/mM (n=3 replicate sensors) and an average response time (t_{95}) of 0.88 sec (Fig. 3a&b). Average sensitivity per exposed geometric tip area was 15.0±2.4 mA mM^{-1} cm^{-2}, which is 11-2000 times higher than previously reported glucose microsensors [27; 45; 46]. The lower limit of detection was 10 μM, and the linear range was 0.01 to 17.5 mM glucose with an R^2 value of 0.99. This linear range spans the expected glucose concentration in tissue culture media (typically 0.5-11.1 mM). Bionanocomposite sensors were stable for up to 7 days when stored in 50 mg GOx/ml PBS at 4°C (less than 1% reduction in sensitivity up to day two; 11% reduction in sensitivity after day seven mainly due to GOx degradation caused by the H_2O_2 produced from glucose oxidation [47]). Although design schemes for glucose biosensors vary depending on application [25; 45], the design used here is simple, robust, and can be used under physiological conditions.

To validate the use of the bionanocomposite sensor in the SR modality, glucose flux was measured in a known glucose concentration gradient within sterile RPMI media (Fig. 3c). The sensor was oscillated at a frequency of 0.3 Hz with an excursion distance of 30 μm (approximately 1.3 sec acquisition time at each position). Based on the measured concentration values near the pipette tip filled with 3mM glucose, an empirical Fickian diffusion model was developed [34] and the correlation between predicted and measured flux was 0.99; the value of the molecular diffusion coefficient for glucose used was 1.5×10^{-6} cm^2 sec^{-1} [48]. The Fickian transport model did not include convection terms, thus the correlation between predicted and measured values ensured that the solution was not stirred by oscillating the sensor (oscillation of SR microsensors in the 0.2-0.4Hz range was also verified by [40]). This abiotic experiment validated the use of the SR bionanocomposite sensor for measuring glucose flux under physiological conditions (37°C in RPMI culture media).

Glucose uptake in pancreatic β cells

Calibrated bionanocomposite sensors were positioned at the surface of INS 1 cell clusters and glucose flux was measured for 60 min. The mean influx at the cell surface (5.9±1.4 μmol cm^{-2} sec^{-1}) was significantly larger than a background measurement (0.28±0.1 pmol cm^{-2} sec^{-1}) ($p<0.01$, $\alpha=0.05$). Regular oscillatory glucose transport with an average oscillation period of 2.9±0.6 min was measured (n=12 replicate confluent cultures) (Fig. 4a).

A simple harmonic oscillator model was developed for describing the average transport in 12 replicate confluent cell clusters: $J=J_0+a*\sin(2\pi/T)*t$, where J=glucose influx, J_0=mean glucose influx (6.41 μmol cm^{-2} sec^{-1}), a=average amplitude of glucose oscillations (1.75 μmol cm^{-2} sec^{-1}), T=average period of oscillation (2.9 min), and t=time. To quantify the regularity of glucose oscillation, the correlation coefficient between average oscillatory glucose flux and the simple harmonic transport model was determined to be 0.78 based on standard statistical approach (Fig. 4b). For the first time, we report a consistent oscillation pattern in glucose uptake (influx) in β cells which is consistent with previous measurements of oscillatory O_2 uptake in HIT β cells (average period 3.1±0.1 min) [11], cytosolic Ca^{2+} concentration (average period 4.6±0.2 min) [3], ATP/ADP ratio (average period around 3 min) [14], and 5-HT/insulin secretion from single islets (average period 3.2±1.2 min) [13]. Comparison studies on oscillatory glucose transport for various β cell lines/islets are underway. Preliminary results showed regular oscillatory patterns for primary islets (supplemental Fig. S1). The oscillation patterns for various cell lines/islets will be investigated in follow-up studies.

Glucose uptake initiates the insulin secretion pathway [3], and is correlated to metabolism via the electron transport chain [49]. Oxygen uptake and insulin secretion are regulated via a transmembrane feedback control system involving cytosolic ATP/ADP ratio and Ca^{2+} concentrations, and membrane bound pumps and channels [3; 12; 49]. Thus, one would expect glucose influx to follow a regular oscillatory pattern similar to other oscillations. Although previous measurements reported oscillations in glucose concentration in single islets [27], these sensors were used invasively, which potentially damaged the cells. In contrast, the *in vitro* technique used in this study was non-invasive at the cell membrane level. To prove this, we performed confocal imaging to evaluate cellular status after SR measurements to show active intracellular esterase activity (stained green) (Fig. 4c) and observed no signs of damaged membranes (otherwise stained red), confirming the non-invasive nature of the SR technique. Since the biosensors did not damage cell membranes, the functionality of the cells was not affected by measurements. In addition, when the glucose concentration in the perfusion media was changed in previous studies [27], approximately 7.4 minutes were required for steady-state concentration measurements due to glucose diffusion and constant consumption by islets. This represented a significant delay for the output signal representing concentration as reported by [27]. In fact, it is common for living organisms to create drift in concentration measurements because of the constant biological consumption of glucose, as in [27], resulting in temporal inaccuracy of the reported measurements. Sometimes the drift was so significant that the signal reflecting physiological change was submerged. Such drift was eliminated by self-referencing biosensors due to the differential concentration measurements and DC coupling [33]. As a result, the output signal of self-referencing glucose biosensors represents the real-time glucose transport in β cells, islets, and other living organisms [32]. This is a major technological improvement for self-referencing biosensors over concentration biosensors.

Another key limitation in previous studies is that measurements made using concentration domain microsensors are not capable of directly quantifying glucose flux due to limitations in spatiotemporal resolution [30; 33; 50]. At the extracellular interface, cell/tissue transport is a function of (i) molecular diffusion (driven by concentration gradients) and (ii) active

transmembrane transport (regulated by metabolism, pumps, and channels); techniques such as SR are required for discriminating between the two types of transport [30]. Previous attempts at measuring transmembrane glucose transport using the SR microsensor technique did not report oscillatory behavior [45], which we attribute to relatively low temporal resolution, low sensitivity, and use of an AC-coupled electronic scheme.

Pharmacology

To test the dependence of oscillatory transport on glucose concentration, excess glucose dissolved in growth media was added to the tissue culture dish after at least three successive oscillations. We found that adding 0.1 mM glucose did induce a transient metabolic response that increased glucose influx by an average of 70±8% (Fig. 5a). However, this was a transient effect and no oscillatory influx patterns were measured during the "peak" stimulation, which had an average flux of 20.8±2.2 μmol cm^{-2} sec^{-1}, and lasted approximately 9.1±0.8 minutes. Approximately 6.5±0.4 min after this peak stimulus, uptake decreased to basal levels, and returned to the nominal baseline oscillating state.

In experiments where we stimulated the cells with 15 mM glucose, peak stimulated glucose uptake was as high as 31.3±4.2 μmol cm^{-2} sec^{-1} and lasted for an average of 12.1±0.2 min, during which time no oscillatory transport was measured (Fig. 5b). The peak value and duration of flux following addition of 15 mM glucose was significantly higher than that following addition of 0.1 mM glucose ($p=0.013$, $\alpha=0.05$). This temporal trend in peak duration was expected, as data suggests saturation of transporters at glucose concentrations of 15mM, but not at 0.1mM [20]. Following this transitory increase, mean glucose flux (18.9±1.8 μmol cm^{-2} sec^{-1}) was significantly higher than basal levels (4.6 μmol cm^{-2} sec^{-1}) ($p<0.01$, $\alpha=0.05$, $n=12$). The oscillation period before glucose stimulation (3.1±0.2 min) was not significantly different than after stimulation (3.3±0.3 min) ($\alpha=0.05$, $n=12$). Addition of excess glucose above 15 mM did not cause a significant difference in mean uptake (Fig. 5c), which was in accordance with the maximum stimulus concentration determined by Porterfield et al. measuring oxygen [11]. The GLUT transport proteins have been shown to follow Michaelis-Menten type kinetics. Based on the average flux after each glucose stimulation, the apparent K_m value for INS 1 cells was calculated to be 6.1±1.5 mM, which was different from reported K_m for GLUT2 (17 mM) or GLUT9 (1.6 mM) [20]. The results indicated that glucose transport in β cells may be facilitated by more than one transporter, and the saturation of transporters with relatively low K_m values may biologically affect transporters with high K_m values. Thus, inhibition experiments targeting specific transporters in knock-out mice are necessary to determine the types of transporter involved.

To abolish metabolic glucose uptake by β cells after stimulus (internal negative control), 10 mM KCN was added to each dish and mixed with a transfer pipette. KCN is a known inhibitor of oxidative phosphorylation and inhibits cytochrome c oxidase via the heme a3-Cu_B center [51]. Within 3 minutes, 10 mM KCN decreased glucose uptake by 99.1±0.4% and no oscillations were observed for any of the replicates (n=6) (Fig. 6a&b). To validate that cells were indeed metabolically inactive, 0.1 mM glucose was again added to the dish and no significant flux was recorded for any cluster replicates (indicating no active biological uptake of the added glucose) (Fig. 6a&b). These stimulation-inhibition experiments clearly indicated that the measured glucose flux at the surface of INS 1 clusters was due to mitochondrial cell respiration.

Phloretin is a known competitive class I GLUT inhibitor, which includes GLUT1 [52] and GLUT2 [53] in mammalian cells. In a separate set of pharmacological experiments, activity of class I GLUT proteins was inhibited by adding phloretin. A dose-response plot for phloretin inhibition (using glucose flux as the activity assay) is presented in Fig. 7a. The calculated EC_{50} value was 28±1.6 μM-phloretin, and the concentration which caused

maximum inhibition was 40±0.6 μM-phloretin. To our knowledge, there have been no previous studies reporting the EC50 value for phloretin with INS 1 cells.

A representative example of a real-time response experiment demonstrates the effects of phloretin on glucose flux oscillations. After addition of 40 μM phloretin, glucose influx was reduced by 64±9% and the oscillatory flux was inhibited (Fig. 7b&c). The phloretin mediated cessation of oscillatory glucose transport could be due to a combination of reduced respiratory ATP production/O_2 influx, and disruption of the feedback cascade triggered by glucose uptake.

Oscillatory metabolism is absent in tissues known to have type 2 diabetes [15] and previous studies showed that impaired glucose transport due to downregulated GLUT2 in β cells was linked to the loss of insulin secretion in type 2 diabetes [54]. By inhibiting GLUT2 via phloretin, we observed the loss of oscillatory transport at the physiological scale, suggesting that impaired GLUT2 may be the cause of the absence of oscillations in type 2 diabetes. The residual non-oscillating flux (ca 35% of basal average flux) was likely due to the activity of glucose transport mechanisms which were not inhibited by phloretin (i.e., those which were not categorized as class I GLUT proteins). After exposure to 40μM phloretin, addition of more of this inhibitor (total concentration=80 μM) had no effect on the average glucose flux (Fig. 7b&c); supporting the hypothesis that transporters not inhibited by phloretin were responsible for the remaining non-oscillatory glucose uptake (in addition to passive diffusion). A previous study reported glucose uptake by GLUT2-null β cells, which was not attributed to GLUT1 or GLUT3 [19]. Results from this study suggest that the remaining transport may have been due to non-class I transporters (e.g., GLUT9 [20; 55; 56]), although additional detailed studies are currently underway to investigate this conclusion. Phloretin concentrations below 1 mM have not been shown to inhibit glucose transport for class II GLUT proteins or voltage dependent transporters such as GLUT9 [55], and results from this study suggested that these proteins were capable of uptaking glucose, but were unable to maintain oscillatory transport when GLUT2 were inhibited. Follow-up inhibition studies on GLUT9 with GLUT2 knock-out mice will provide a more definite answer to this question.

To abolish electron transport after the phloretin studies, 10 mM KCN was added to each dish, which completely inhibited glucose influx (n=4) (Fig. 7b&c).

The combination of high porosity and enhanced catalytic activity of the bionanocomposite sensor design allowed us to resolve temporally dynamic oscillations in glucose consumption as theoretically predicted [11; 12; 27]. We attribute the ability to quantify physiological glucose transport in INS 1 cells to the use of highly conductive nanomaterials (enhancing amperometric sensitivity, linear detection range, and effective surface area) and the use of a DC coupled electronic scheme (alleviating capacitive signal decay) [33].

The ability to non-invasively quantify transport in physiological and pathophysiological conditions will improve our understanding of transport processes associated with type 2 diabetes. Previous studies have shown that mutations in the *IPF1/PDX1* gene of β cells may lead to the development of type 2 diabetes, causing impaired expression of GLUT2 and secretion of insulin [21; 57]. Our studies, however, did not use mutated cells. Further studies regarding abnormalities in transport via specific GLUT proteins are underway in an attempt to link the measurements in the physiome to abnormalities in the genome. Studies on the glucose transport activities under various pathophysiological conditions based on this technique will contribute greatly to the understanding of the genetic cause(s) of diabetes and the development of potential therapies.

Supplementary Material

Refer to Web version on PubMed Central for supplementary material.

Acknowledgments

The authors would like to acknowledge Natalie Stull and Dr. Raghu Mirmira, the Wells Center for Pediatric Research, Program in Diabetes Control at Indiana University who harvested murine islets and provided the INS 1 cell line used in this study. This research was partially funded by the National Science Foundation Instrumentation for Biological Research program.

References

[1]. Chou HF, Ipp E. Pulsatile insulin secretion in isolated rat islets. Diabetes. 1990; 39:112–7. [PubMed: 2210053]

[2]. Weigle DS. Pulsatile secretion of fuel-regulatory hormones. Diabetes. 1987; 36:764–75. [PubMed: 3552804]

[3]. Longo EA, Tornheim K, Deeney JT, Varnum BA, Tillotson D, Prentki M, Corkey BE. Oscillations in cytosolic free Ca2+, oxygen consumption, and insulin secretion in glucose-stimulated rat pancreatic islets. Journal of biological chemistry. 1991; 266:9314–9. [PubMed: 1902835]

[4]. Holz GG. Epac: A New cAMP-Binding Protein in Support of Glucagon-Like Peptide-1 Receptor-Mediated Signal Transduction in the Pancreatic b-Cell. Diabetes. 2004; 53:5–13. [PubMed: 14693691]

[5]. Henquin JC. Triggering and amplifying pathways of regulation of insulin secretion by glucose. Diabetes. 2000; 49:1751. [PubMed: 11078440]

[6]. Detimary P, Gilon P, Henquin JC. Interplay between cytoplasmic Ca2+ and the ATP/ADP ratio: a feedback control mechanism in mouse pancreatic islets. Biochem J. 1998; 333:269–274. [PubMed: 9657965]

[7]. Tornheim K. Are metabolic oscillations responsible for normal oscillatory insulin secretion? Diabetes. 1997; 46:1375–80. [PubMed: 9287034]

[8]. Heart E, Smith PJS. Rhythm of the beta-cell oscillator is not governed by a single regulator: multiple systems contribute to oscillatory behavior. Am J Physiol Endocrinol Metab. 2007; 292:E1295. [PubMed: 17213468]

[9]. Henquin J. Regulation of insulin secretion: a matter of phase control and amplitude modulation. Diabetologia. 2009; 52:739–751. [PubMed: 19288076]

[10]. Bertram R, Sherman A, Satin LS. Metabolic and electrical oscillations: partners in controlling pulsatile insulin secretion. Am J Physiol Endocrinol Metab. 2007; 293:E890. [PubMed: 17666486]

[11]. Porterfield DM, Corkey RF, Sanger RH, Tornheim K, Smith PJ, Corkey BE. Oxygen consumption oscillates in single clonal pancreatic beta-cells (HIT). Diabetes. 2000; 49:1511–1516. [PubMed: 10969835]

[12]. Kennedy RT, Kauri LM, Dahlgren GM, Jung S-K. Metabolic Oscillations in b-Cells. Diabetes. 2002; 51:S152–S161. [PubMed: 11815475]

[13]. Barbosa RM, Silva A, Tome A, Stamford JA, Santos AS, Rosario L. Real Time Electrochemical Detection of 5-HT/Insulin Secretion from Single Pancreatic Islets: Effect of Glucose and K +Depolarization. Biochemical and Biophysical Research Communications. 1996; 228:100–104. [PubMed: 8912642]

[14]. Nilsson T, Schultz V, Berggren PO, Corkey BE, Tornheim K. Temporal patterns of changes in ATP/ADP ratio, glucose 6-phosphate and cytoplasmic free Ca2+ in glucose-stimulated pancreatic beta-cells. Biochemical journal. 1996; 314:91–4. [PubMed: 8660314]

[15]. Weigle DS. Pulsatile secretion of fuel-regulatory hormones. Diabetes. 1987; 36:764. [PubMed: 3552804]

[16]. O'Rahilly S, Turner RC, Matthews DR. Impaired pulsatile secretion of insulin in relatives of patients with non-insulin-dependent diabetes. N Engl J Med. 1988; 318:1225–1230. [PubMed: 3283553]

[17]. Polonsky KS, Given BD, Hirsch LJ, Tillil H, Shapiro ET, Beebe C, Frank BH, Galloway JA, Van Cauter E. Abnormal Patterns of Insulin Secretion in Non-Insulin-Dependent Diabetes Mellitus. New England Journal of Medicine. 1988; 318:1231–1239. [PubMed: 3283554]

[18]. Thorens B, Sarkar HK, Kaback HR, Lodish HF. Cloning and functional expression in bacteria of a novel glucose transporter present in liver, intestine, kidney, and [beta]-pancreatic islet cells. Cell. 1988; 55:281–290. [PubMed: 3048704]

[19]. Guillam MT, Dupraz P, Thorens B. Glucose uptake, utilization, and signaling in GLUT2-null islets. Diabetes. 2000; 49:1485–1491. [PubMed: 10969832]

[20]. Evans SA, Doblado M, Chi MM, Corbett JA, Moley KH. Facilitative Glucose Transporter 9 Expression Affects Glucose Sensing in Pancreatic {beta}-Cells. Endocrinology. 2009; 150:5302–5310. [PubMed: 19808778]

[21]. Ahlgren U, Jonsson J, Jonsson L, Simu K, Edlund H. β-Cell-specific inactivation of the mouseIpf1/Pdx1 gene results in loss of the β-cell phenotype and maturity onset diabetes. Genes & Dev. 1998; 12:1763. [PubMed: 9637677]

[22]. Sweet IR, Li G, Najafi H, Berner D, Matschinsky FM. Effect of a glucokinase inhibitor on energy production and insulin release in pancreatic islets. Am J Physiol Endocrinol Metab. 1996; 271:E606–625.

[23]. Weiss RG, Chacko VP, Glickson JD, Gerstenblith G. Comparative 13C and 31P NMR assessment of altered metabolism during graded reductions in coronary flow in intact rat hearts. Proc Natl Acad Sci USA. 1989; 86:6426–6430. [PubMed: 2762333]

[24]. Moley KH, Chi MMY, Mueckler MM. Maternal hyperglycemia alters glucose transport and utilization in mouse preimplantation embryos. Am J Physiol Endocrinol Metab. 1998; 275:E38–47.

[25]. Claussen JC, Franklin AD, ul Haque A, Porterfield DM, Fisher TS. Electrochemical Biosensor of Nanocube-Augmented Carbon Nanotube Networks. ACS Nano. 2009; 3:37–44. [PubMed: 19206246]

[26]. Abdel-Humid I, Atanasov P, Wilkins E. Needle-type glucose biosensor with an electrochemically codeposited enzyme in a platinum black matrix. Electroanalysis. 1995; 7:738–741.

[27]. Jung S-K, Kauri LM, Qian W-J, Kennedy RT. Correlated Oscillations in Glucose Consumption, Oxygen Consumption, and Intracellular Free Ca2+ in Single Islets of Langerhans. J Biol Chem. 2000; 275:6642–6650. [PubMed: 10692473]

[28]. Hrapovic S, Liu Y, Male KB, Luong JH. Electrochemical biosensing platforms using platinum nanoparticles and carbon nanotubes. Analytical chemistry. 2004; 76:1083–8. [PubMed: 14961742]

[29]. Gong K, Yan Y, Zhang M, Su L, Xiong S, Mao L. Electrochemistry and Electroanalytical Applications of Carbon Nanotubes: A Review. ANALYTICAL SCIENCES. 2005; 21:1383–1394. [PubMed: 16379375]

[30]. McLamore ES, Mohanty S, Shi J, Claussen J, Jedlicka SS, Rickus JL, Porterfield DM. A self-referencing glutamate biosensor for measuring real time neuronal glutamate flux. Journal of Neuroscience Methods. 2010; 189:14–22. [PubMed: 20298719]

[31]. Jaffe LF, Nuccitelli R. AN ULTRASENSITIVE VIBRATING PROBE FOR MEASURING STEADY EXTRACELLULAR CURRENTS. J Cell Biol. 1974; 63:614–628. [PubMed: 4421919]

[32]. McLamore ES, Shi J, Jaroch D, Claussen J, Uchida A, Jiang YJ, Banks MK, Buhman KK, Teegarden D, Rickus JL, Porterfield DM. A self referencing platinum nanoparticle decorated enzyme-based microbiosensor for real time measurement of physiological glucose transport. Biosensors & Bioelectronics. 2010 in press.

[33]. Porterfield DM. Measuring metabolism and biophysical flux in the tissue, cellular and subcellular domains: Recent developments in self-referencing amperometry for physiological sensing. Biosensors and Bioelectronics. 2007; 22:1186–1196. [PubMed: 16870420]

[34]. McLamore ES, Porterfield DM, Banks MK. Non-Invasive Self-Referencing Electrochemical Sensors for Quantifying Real-Time Biofilm Analyte Flux. Biotechnology and bioengineering. 2009:791–799. [PubMed: 18985610]

[35]. Chatni MR, Porterfield DM. Self-referencing optrode technology for non-invasive real-time measurement of biophysical flux and physiological sensing. Analyst. 2009; 134:2224–2232. [PubMed: 19838408]

[36]. Porterfield DM, McLamore ES, Banks MK. Microsensor technology for measuring H+ flux in buffered media. Sensors and Actuators B: Chemical. 2009; 136:383–387.

[37]. Zuberi M, Liu-Snyder P, ul Haque A, Porterfield D, Borgens R. Large naturally-produced electric currents and voltage traverse damaged mammalian spinal cord. J Biol Eng. 2008; 2:17. [PubMed: 19116024]

[38]. McLamore ES, Diggs A, Marzal P. Calvo, Shi J, Blakeslee JJ, Peer WA, Murphy AS, Porterfield DM. Non-invasive quantification of endogenous root auxin transport using an integrated flux microsensor technique. The Plant Journal. 2010 in press.

[39]. Hohmeier HE, Mulder H, Chen GX, Henkel-Rieger R, Prentki M, Newgard CB. Isolation of INS-1-derived cell lines with robust ATP-sensitive K+ channel-dependent and -independent glucose-stimulated insulin secretion. Diabetes. 2000; 49:424–430. [PubMed: 10868964]

[40]. Kuhtreiber WM, Jaffe LF. Detection of Extracellular Calcium Gradients with a Calcium-Specific Vibrating Electrode. Journal of Cell Biology. 1990; 110:1565–1573. [PubMed: 2335563]

[41]. Heinze J. Ultramicroelectrodes in Electrochemistry. J. Angew. Chem., Int. Ed. Engl. 1993; 32:1268–1288.

[42]. Wang J, Musameh M, Lin Y. Solubilization of carbon nanotubes by Nafion toward the preparation of amperometric biosensors. Journal of the American Chemical Society. 2003; 125:2408–9. [PubMed: 12603125]

[43]. Wang SG, Zhang Q, Wang R, Yoon SF, Ahn J, Yang DJ, Tian JZ, Li JQ, Zhou Q. Multi-walled carbon nanotubes for the immobilization of enzyme in glucose biosensors. Electrochemistry Communications. 2003; 5:800–803.

[44]. McMahon CP, Rocchitta G, Serra PA, Kirwan SM, Lowry JP, O'Neill RD. Control of the Oxygen Dependence of an Implantable Polymer/Enzyme Composite Biosensor for Glutamate. Analytical Chemistry. 2006; 78:2352–2359. [PubMed: 16579619]

[45]. Jung S-K, Trimarchi JR, Sanger RH, Smith PJS. Development and Application of a Self-Referencing Glucose Microsensor for the Measurement of Glucose Consumption by Pancreatic B-Cells. Analytical Chemistry. 2001; 73:3759–3767. [PubMed: 11510845]

[46]. Kohma T, Oyamatsu D, Kuwabata S. Preparation of selective micro glucose sensor without permselective membrane by electrochemical deposition of ruthenium and glucose oxidase. Electrochemistry Communications. 2007; 9:1012–1016.

[47]. Valdes TI, Moussy F. In vitro and in vivo degradation of glucose oxidase enzyme used for an implantable glucose biosensor. Diabetes Technology & Therapeutics. 2000; 2:367–376. [PubMed: 11467339]

[48]. Converti A, Casagrande M, De Giovanni M, Rovatti M, Del Borghi M. Evaluation of glucose diffusion coefficient through cell layers for the kinetic study of an immobilized cell bioreactor. Chemical Engineering Science. 1996; 51:1023–1026.

[49]. Henquin JC. Glucose-induced electrical activity in beta-cells. Feedback control of ATP-sensitive K+ channels by Ca2+ Diabetes. 1990; 39:1457–1460. [PubMed: 2227118]

[50]. Kochian LV, Shaff JE, Kühtreiber WM, Jaffe LF, Lucas WJ. Use of an extracellular, ion-selective, vibrating microelectrode system for the quantification of K+, H+, and Ca 2+ fluxes in maize roots and maize suspension cells. Planta. 1992; 188:601–610.

[51]. Way JL. Cyanide Intoxication and its Mechanism of Antagonism. Annu Rev Pharmacol Toxicol. 1984; 24:451–481. [PubMed: 6428300]

[52]. Dominguez JH, Soleimani M, Batiuk T. Studies of renal injury IV: The GLUT1 gene protects renal cells from cyclosporine A toxicity. Kidney Int. 2002; 62:127–136. [PubMed: 12081571]

[53]. Kellett GL, Helliwell PA. The diffusive component of intestinal glucose absorption is mediated by the glucose-induced recruitment of GLUT2 to the brush-border membrane. Biochem J. 2000; 350:155–162. [PubMed: 10926839]

[54]. Unger RH. Diabetic hyperglycemia: link to impaired glucose transport in pancreatic beta cells. Science. 1991; 251:1200. [PubMed: 2006409]

[55]. Caulfield MJ, Munroe PB, O'Neill D, Witkowska K, Charchar FJ, Doblado M, Evans S, Eyheramendy S, Onipinla A, Howard P, Shaw-Hawkins S, Dobson RJ, Wallace C, Newhouse SJ, Brown M, Connell JM, Dominiczak A, Farrall M, Lathrop GM, Samani NJ, Kumari M, Marmot M, Brunner E, Chambers J, Elliott P, Kooner J, Laan M, Org E, Veldre G, Viigimaa M, Cappuccio FP, Ji C, Iacone R, Strazzullo P, Moley KH, Cheeseman C. SLC2A9 Is a High-Capacity Urate Transporter in Humans. PLoS Medicine. 2008; 5:e197. [PubMed: 18842065]

[56]. Bibert S, Hess S. Kharoubi, Firsov D, Thorens B, Geering K, Horisberger JD, Bonny O. Mouse GLUT9: evidences for a urate uniporter. American Journal of Physiology- Renal Physiology. 2009 00139.2009.

[57]. Moibi JA, Gupta D, Jetton TL, Peshavaria M, Desai R, Leahy JL. Peroxisome Proliferator-Activated Receptor- Regulates Expression of PDX-1 and NKX6. 1 in INS-1 Cells. Diabetes. 2007; 56:88. [PubMed: 17192469]

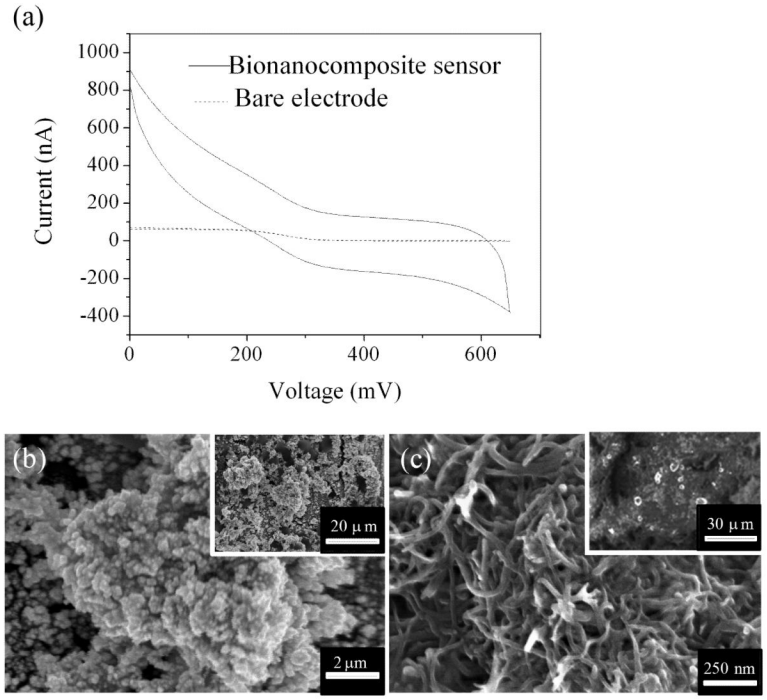

Fig. 1.

(a) CV in 4 mM $Fe(CN)_6^{3-}$/1M KNO_3 for a bare micro electrode and a bionanocomposite sensor at a scan rate 20mV/s. Representative surface morphology determined by FESEM for the tip of bionanocomposite sensors after sequential electrodeposition of (b) Pt black, and (c) a MWNT/Nafion layer (insets demonstrate typical low magnification images).

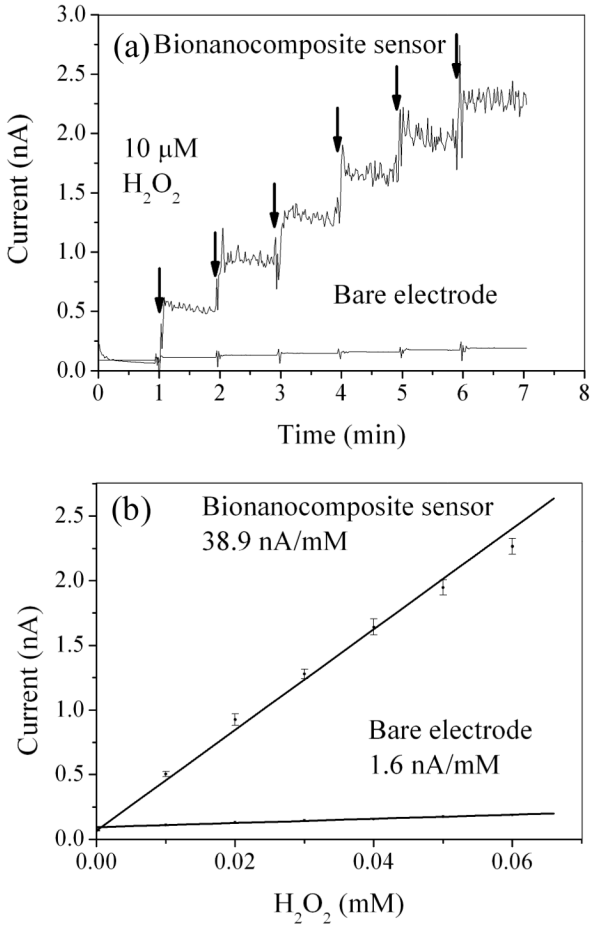

Fig. 2.

(a) Representative current response to H_2O_2 for a bionanocomposite sensor and a bare electrode. (b) Average linear regression result for averaged current versus molar concentration of H_2O_2.

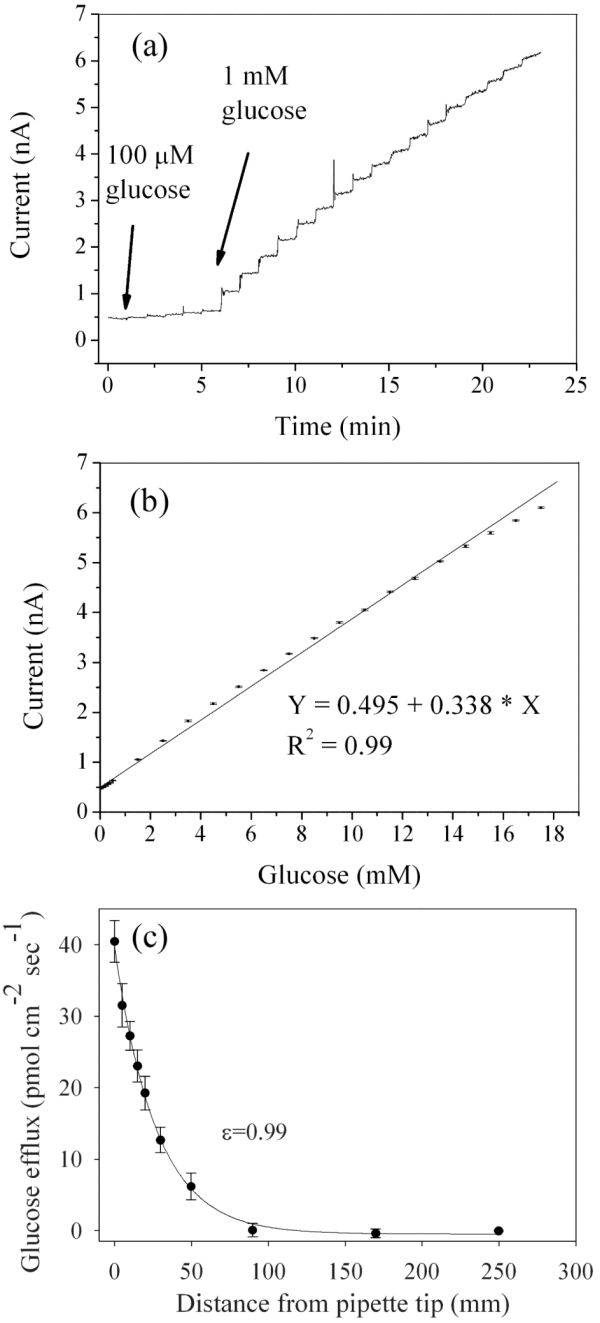

Fig. 3.

(a) Representative current response for a bionanocomposite sensor when glucose concentration increased from 0.1 to 17.5 mM. (b) Average linear regression for averaged current versus molar concentration of glucose. (c) Abiotic step back experiment from pulled micropipette containing 3 mM glucose and 0.5% agar in PBS at 37°C. Correlation coefficient (ε) between measured (•) and predicted flux (solid line) was 0.99. All error bars represent the standard error of the arithmetic mean.

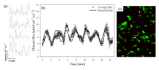

Fig. 4.

(a) Representative oscillatory glucose flux in four replicate confluent INS 1 clusters out of 12 total. Average oscillation period (indicated by a vertical dashed line) was 2.9±0.6 min (n=12). (b) Average glucose flux (dots, n=12 replicate confluent INS 1 cells) and harmonic oscillator model (solid line): $J=J_0+a*\sin(2\pi/T)\ ^{*}t$ (a=1.75 μmol cm^{-2} sec^{-1}, T=2.9 min, J_0=6.41 μmol cm^{-2} sec^{-1}). Average basal glucose influx in cultured β cell (INS 1) clusters was 5.9±1.4 μmol cm^{-2} sec^{-1} (n=12). Correlation coefficient between modeled and measured data was 0.78. (c) Representative confocal microscopy image of INS 1 cells using a viability stain (Cell tracker); green fluorescence indicates live cells (esterase activity), and red fluorescence indicates dead cells (propidium iodine).

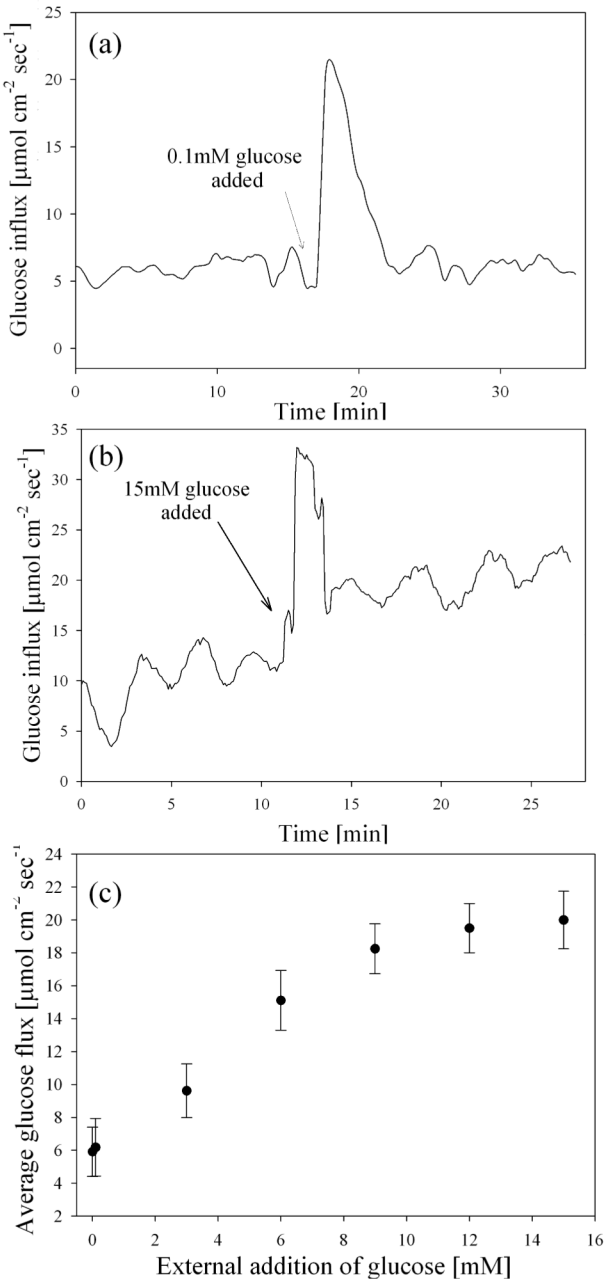

Fig. 5.

a). Representative glucose flux measured at the surface of cultured INS 1 β cells during stimulation with 0.1 mM glucose. Three successive oscillations were measured under basal conditions (average period was 3.1±0.3 min), and cells were then stimulated by adding cell culture media with excess glucose (total glucose concentration increased by 0.1mM). (b) Representative glucose flux during stimulation with 15 mM glucose. (c) Dose-response analysis of glucose flux in response to stimulation via excess addition of glucose (error bars represent standard deviation of the arithmetic mean). The maximum glucose concentration which caused a stimulatory response (15 mM) is consistent with previous glucose dose-response analysis of O_2 flux into HIT β cells [11].

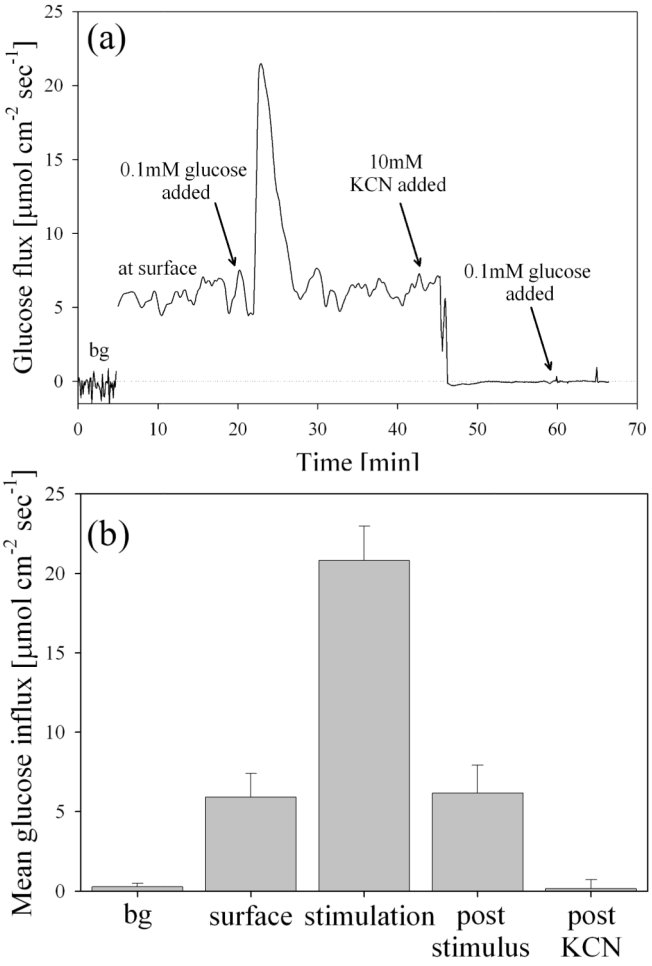

Fig. 6.

(a) Following a background measurement (bg), five successive oscillations were measured (noted as "*at surface*") prior to stimulation with 0.1mM glucose. After stimulation with 0.1mM glucose (noted as "*stimulation*"), five oscillations were again measured (noted as *post-stimulus*) prior to inhibition of electron transport by addition of 10mM KCN (noted as *post-KCN*). (b) Average data during stimulation-inhibition experiments in part a (n=12 replicate confluent clusters). Oscillation period before glucose stimulation (3.1±0.5 min) was not significantly different than after stimulation (3.3±0.3 min) ($p<0.01$, $\alpha=0.05$).

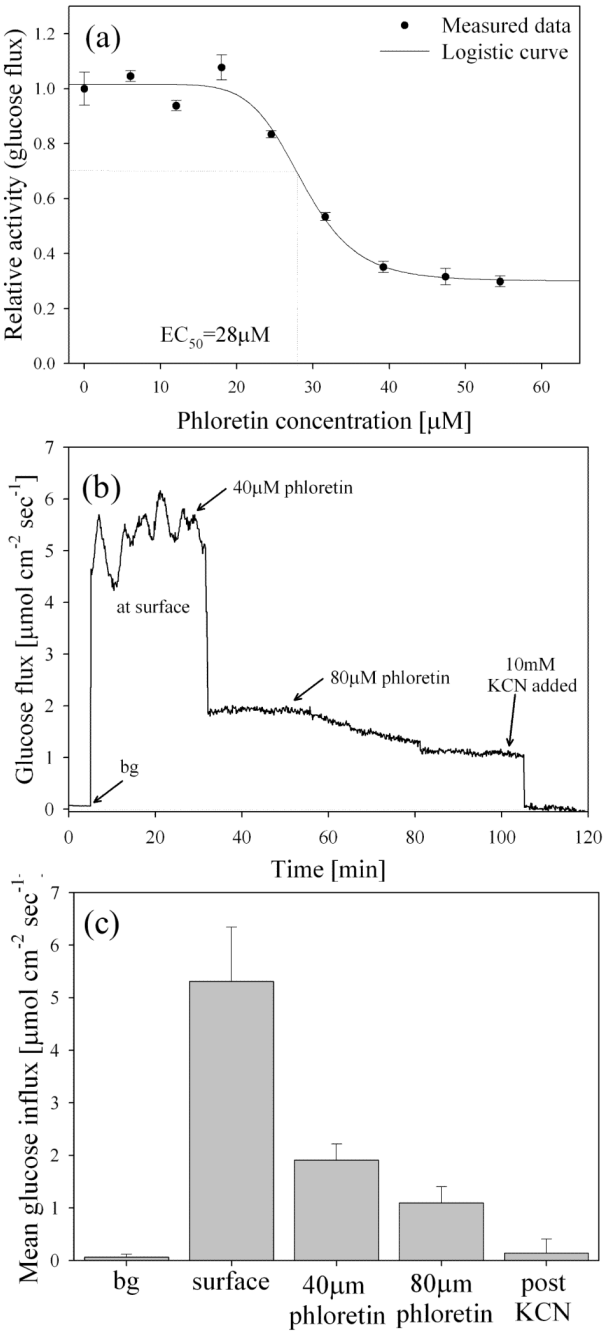

Fig. 7.

a) Dose-response plot for phloretin inhibition using glucose flux as the activity assay. The calculated EC_{50} value was 28±1.6 μM-phloretin, and the concentration which caused maximum transport inhibition was 40 μM-phloretin. All error bars represent the standard deviation of the arithmetic mean (n=3 replicate confluent clusters). (b) Representative glucose flux measured at the surface of cultured INS 1 β cells during inhibition by external addition of phloretin. A minimum of three successive oscillations were measured under basal conditions (average period was 2.9±0.4 min), and glucose transport was then inhibited by addition of 40 μM phloretin and 80 μM phloretin (total concentration noted). Glucose transport was subsequently abolished via addition of 10 mM KCN. (c) Mean glucose uptake

decreased by an average of 64±9% following addition of 40 μM phloretin, and by 79.4±6% in the presence of 80 μM phloretin. No oscillations were measured following the addition of 40 μM phloretin, and mean flux following addition of 10mM KCN was not significantly different from background measurements ($p<0.01$, $\alpha=0.05$). All error bars represent the standard deviation of the arithmetic mean.